



# Zoledronic acid renders human M1 and M2 macrophages susceptible to V $\delta$ 2<sup>+</sup> $\gamma$ $\delta$ T cell cytotoxicity in a perforin-dependent manner

Daniel W. Fowler<sup>1</sup>  · John Copier<sup>1</sup> · Angus G. Dalgleish<sup>1</sup> · Mark D. Bodman-Smith<sup>1</sup>Received: 16 January 2017 / Accepted: 2 May 2017 / Published online: 13 May 2017  
© The Author(s) 2017. This article is an open access publication

**Abstract** V $\delta$ 2<sup>+</sup> T cells are a subpopulation of  $\gamma$  $\delta$  T cells in humans that are cytotoxic towards cells which accumulate isopentenyl pyrophosphate. The nitrogen-containing bisphosphonate, zoledronic acid (ZA), can induce tumour cell lines to accumulate isopentenyl pyrophosphate, thus rendering them more susceptible to V $\delta$ 2<sup>+</sup> T cell cytotoxicity. However, little is known about whether ZA renders other, non-malignant cell types susceptible. In this study we focussed on macrophages (M $\phi$ s), as these cells have been shown to take up ZA. We differentiated peripheral blood monocytes from healthy donors into M $\phi$ s and then treated them with IFN- $\gamma$  or IL-4 to generate M1 and M2 M $\phi$ s, respectively. We characterised these M $\phi$ s based on their phenotype and cytokine production and then tested whether ZA rendered them susceptible to V $\delta$ 2<sup>+</sup> T cell cytotoxicity. Consistent with the literature, IFN- $\gamma$ -treated M $\phi$ s expressed higher levels of the M1 markers CD64 and IL-12p70, whereas IL-4-treated M $\phi$ s expressed higher levels of the M2 markers CD206 and chemokine (C–C motif) ligand 18. When treated with ZA, both M1 and M2 M $\phi$ s became susceptible to V $\delta$ 2<sup>+</sup> T cell cytotoxicity. V $\delta$ 2<sup>+</sup> T cells expressed perforin and degranulated in response to ZA-treated M $\phi$ s as shown by mobilisation of CD107a and CD107b to the cell surface. Furthermore, cytotoxicity towards ZA-treated M $\phi$ s was sensitive—at least in part—to

the perforin inhibitor concanamycin A. These findings suggest that ZA can render M1 and M2 M $\phi$ s susceptible to V $\delta$ 2<sup>+</sup> T cell cytotoxicity in a perforin-dependent manner, which has important implications regarding the use of ZA in cancer immunotherapy.

**Keywords**  $\gamma$  $\delta$  T cell · V $\delta$ 2<sup>+</sup> T cell · Macrophage · Zoledronic acid · Cytotoxicity

## Abbreviations

|          |  |
|----------|--|
| CCL      | Chemokine (C–C motif) ligand             |
| CFSE     | Carboxyfluorescein succinimidyl ester    |
| CMA      | Concanamycin A                           |
| FSC      | Forward scatter                          |
| G        | Gate                                     |
| IPP      | Isopentenyl pyrophosphate                |
| LSD      | Least significant difference             |
| M $\phi$ | Macrophage                               |
| MFI      | Mean (arithmetic) fluorescence intensity |
| NBP      | Nitrogen-containing bisphosphonate       |
| SD       | Standard deviation                       |
| SSC      | Side scatter                             |
| TAM      | Tumour-associated macrophage             |
| ZA       | Zoledronic acid                          |

## Introduction

Human peripheral blood contains a subpopulation of  $\gamma$  $\delta$  T cells that express TCRs composed of V $\gamma$ 9 and V $\delta$ 2 subunits. These cells—referred to here as V $\delta$ 2<sup>+</sup> T cells—typically represent 0.5–5% of peripheral blood T cells and exert potent cytotoxicity against their target cells.

V $\delta$ 2<sup>+</sup> T cells detect intermediates of isoprenoid biosynthesis, namely isopentenyl pyrophosphate (IPP) and

**Electronic supplementary material** The online version of this article (doi:10.1007/s00262-017-2011-1) contains supplementary material, which is available to authorized users.

✉ Daniel W. Fowler  
dfowler@sgul.ac.uk

<sup>1</sup> Institute for Infection and Immunity, St. George's University of London, Cranmer Terrace, Tooting, London SW17 0RE, UK

(E)-4-hydroxy-3-methyl-but-2-enyl pyrophosphate. IPP is generated by the endogenous mevalonate pathway as well as the exogenous 1-deoxy-D-xylulose-5-phosphate pathway, whereas (E)-4-hydroxy-3-methyl-but-2-enyl pyrophosphate is generated by the 1-deoxy-D-xylulose-5-phosphate pathway only [1]. The mevalonate pathway is often dysregulated in malignant and infected cells, resulting in accumulation of IPP and increased susceptibility to V $\delta$ 2<sup>+</sup> T cell cytotoxicity [2, 3]. Moreover, certain cells accumulate IPP when exposed to the nitrogen-containing bisphosphonate (NBP), zoledronic acid (ZA) [4], a synthetic drug that inhibits an enzyme of the mevalonate pathway called farnesyl pyrophosphate synthase [5]. Although the precise mechanism of IPP and (E)-4-hydroxy-3-methyl-but-2-enyl pyrophosphate recognition by V $\delta$ 2<sup>+</sup> T cells has yet to be determined, evidence suggests that it is TCR dependent and involves butyrophilin 3A1 [6].

Zoledronic acid is typically used to treat complications associated with excessive bone resorption in diseases such as osteoporosis, Paget's disease and metastatic bone disease [7]. In terms of its mode of action, ZA binds to bone and disrupts the activity of bone remodelling cells called osteoclasts [8]. ZA also has potential as an immunotherapy for cancer, the proof of concept for which has already been demonstrated in clinical trials [9–11]. Although in cancer its mode of action is poorly understood, experiments *in vitro* have shown that tumour cell lines from a broad range of haematological and solid malignancies become more susceptible to V $\delta$ 2<sup>+</sup> T cell cytotoxicity when exposed to ZA, suggesting a role for V $\delta$ 2<sup>+</sup> T cells [12–14]. However, the capacity for ZA to induce susceptibility in other, non-malignant cell types is poorly characterised and could provide insight that helps to better understand the effects of this drug and improve its clinical application. In this study we have focussed on macrophages (denoted here as M $\phi$ s) because these cells have been shown recently to take up NBPs *in vivo* [15] and are implicated in the progression of cancer [16].

M $\phi$ s are tissue-resident phagocytic cells that play a critical role in tissue repair as well as immunity against pathogenic infection and malignant transformation [17]. M $\phi$ s display functional plasticity that is intricately linked to their surrounding microenvironment [18]. Researchers have categorised the different functional states of M $\phi$ s according to their capacity to either promote inflammation or suppress it. At one end of the spectrum are pro-inflammatory M $\phi$ s, also referred to as M1 or classically activated M $\phi$ s, and at the other end are anti-inflammatory M $\phi$ s, also known as M2 or alternatively activated M $\phi$ s [19]. IFN- $\gamma$  and IL-4 have been identified as key drivers of these opposing M1 and M2 phenotypes, respectively [19].

As part of our ongoing studies into how ZA stimulates anti-tumour responses in V $\delta$ 2<sup>+</sup> T cells, we identified a

previously unexplored effect involving V $\delta$ 2<sup>+</sup> T cell targeting of myeloid cells. Recently, we showed that ZA can render peripheral blood monocytes susceptible to V $\delta$ 2<sup>+</sup> T cell cytotoxicity *in vitro* [20]. In a subsequent study by Junankar et al., tumour-associated M $\phi$ s (TAMs) in breast cancer were identified as important targets for NBPs *in vivo* [15]. Therefore, we further explored the concept of V $\delta$ 2<sup>+</sup> T cell targeting of myeloid cells, and found that ZA can render M1 and M2 M $\phi$ s susceptible to V $\delta$ 2<sup>+</sup> T cell cytotoxicity. Furthermore, we found that V $\delta$ 2<sup>+</sup> T cell cytotoxicity towards ZA-treated M $\phi$ s was dependent—at least in part—on perforin. This novel insight into the interplay between V $\delta$ 2<sup>+</sup> T cells and M $\phi$ s has important implications regarding the use of ZA in cancer immunotherapy.

## Materials and methods

### PBMC isolation

Anonymised leukocyte cones from healthy donors were obtained from the National Health Service blood transfusion unit at St. George's Hospital, London. PBMCs were isolated by density-adjusted centrifugation using Histopaque-1077 (Sigma-Aldrich). RBCs were lysed with ammonium chloride solution and platelets removed by slow-speed centrifugation. PBMCs were resuspended at  $2 \times 10^7$  cells/ml of freezing medium (45% RPMI-1640, 45% FBS and 10% DMSO; all from Sigma-Aldrich) and frozen at  $-80^\circ\text{C}$  in Mr Frosty freezing containers (Thermo Scientific) prior to transferring them to liquid nitrogen.

### Cell culture

All cell culture was carried out in a humidified incubator at  $37^\circ\text{C}$  with 5% CO<sub>2</sub>. To generate M $\phi$ s, monocytes were isolated from PBMCs using CD14 microbeads according to the manufacturer's instructions (Miltenyi Biotec). Monocytes were resuspended in serum-free medium (RPMI-1640 containing 2 mM L-glutamine, 100 units/ml penicillin and 100  $\mu\text{g/ml}$  streptomycin; all from Sigma-Aldrich) at a density of  $3.8 \times 10^5$  cells/ml, and 200  $\mu\text{l}$ , 2 or 5 ml of cell suspension added per well of 96-well, 12-well or 6-well tissue culture plates, respectively (Thermo Scientific). Monocytes were cultured for 2 h, after which time the majority of cells were adherent to the tissue culture plate. This process is known to activate monocytes and initiate the macrophage colony-stimulating factor production required for M $\phi$  differentiation [21]. The adherent monocytes were then cultured for 10 days in complete medium (RPMI-1640 containing 10% FBS, 2 mM L-glutamine, 100 units/ml penicillin and 100  $\mu\text{g/ml}$  streptomycin), after which time the monocytes had differentiated into M $\phi$ s, as indicated by

the morphological changes and plastic adherence observed using light microscopy. M1 and M2 M $\phi$ s were generated by adding 25 ng/ml of recombinant human IFN- $\gamma$  or IL-4 (R and D Systems), respectively, on day 7. M $\phi$ s that had not been treated with IFN- $\gamma$  or IL-4 (designated M0s) were used as controls throughout. 10  $\mu$ M ZA (Sigma-Aldrich) was added to the M $\phi$ s on day 9. To generate pure populations of V $\delta$ 2<sup>+</sup> T cells, PBMCs were resuspended at  $2 \times 10^6$  cells/ml of complete medium containing 1  $\mu$ M ZA and 5 ng/ml recombinant human IL-2 (R and D Systems), and 250  $\mu$ l of cell suspension added per well of 96-well round-bottomed tissue culture plates (Thermo Scientific). The cells were cultured for 9 days and fed every 2–3 days with fresh medium containing 5 ng/ml IL-2. Dead cells and non- $\gamma\delta$  T cells were depleted sequentially using dead cell removal kits and TCR $\gamma\delta$  negative isolation kits according to the manufacturer's instructions (Miltenyi Biotec). The purity of V $\delta$ 2<sup>+</sup>CD3<sup>+</sup> cells was assessed by flow cytometry using PE-conjugated mouse anti-human V $\delta$ 2 (clone 123R3; Miltenyi Biotec) and PerCP-conjugated mouse anti-human CD3 (clone SK7; Biolegend) or FITC-conjugated mouse anti-human CD3 (clone HIT3a; Becton–Dickinson). For one donor, a high percentage of V $\delta$ 1<sup>+</sup>CD3<sup>+</sup> cells was detected post-isolation, and so V $\delta$ 1<sup>+</sup> cells were depleted

using allophycocyanin-conjugated recombinant human anti-V $\delta$ 1 (clone REA173; Miltenyi Biotec) and anti-allophycocyanin microbeads according to the manufacturer's instructions (Miltenyi Biotec; supplementary Fig. 1). We speculate that this donor's PBMCs had a particularly high percentage of V $\delta$ 1<sup>+</sup> T cells prior to ZA and IL-2 stimulation and/or their V $\delta$ 1<sup>+</sup> T cells underwent bystander expansion in response to ZA and IL-2.

### Flow cytometry

Day 10 M $\phi$ s in six-well tissue culture plates were washed twice in PBS (Sigma-Aldrich) and cultured for 15 min in PBS containing 0.25% trypsin (Life Technologies) and 2 mM EDTA (Sigma-Aldrich). Cells were detached by repeated pipetting and then washed in complete medium to deactivate the trypsin. M $\phi$ s were resuspended in flow cytometry buffer (PBS with 1% BSA and 0.09% sodium azide; all from Sigma-Aldrich) containing either FITC-conjugated mouse anti-human CD64 (clone 10.1; Becton–Dickinson) or PE-conjugated mouse anti-human CD206 (clone 19.2; Becton–Dickinson). Matched isotype controls were used to determine the amount of background expression. After 10 min at room temperature, cells were

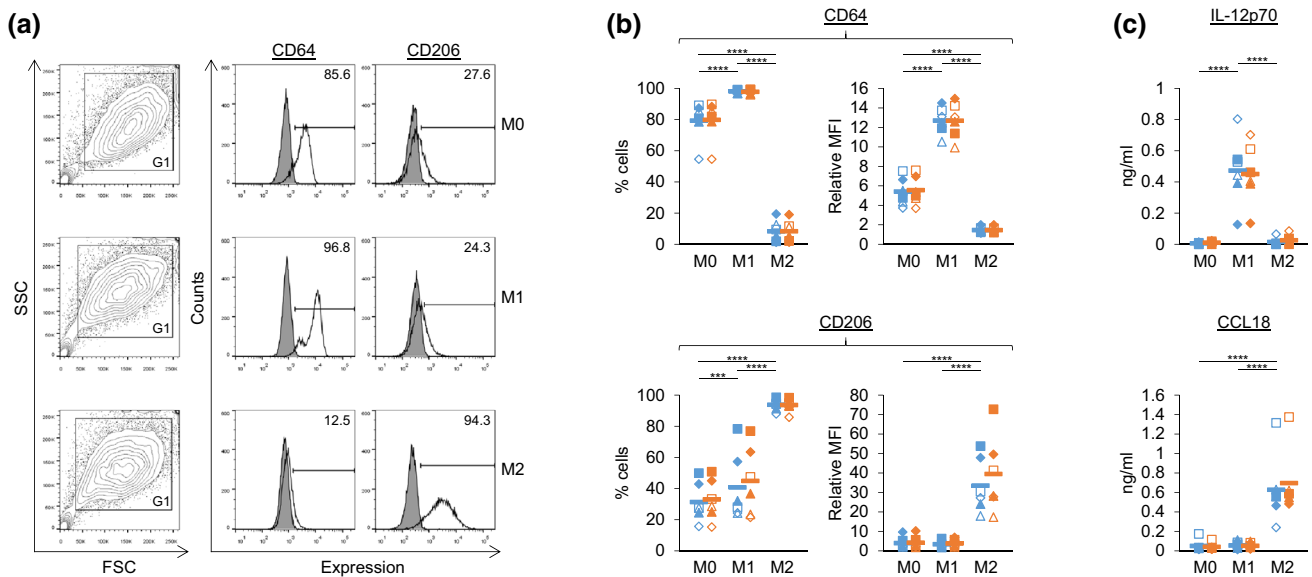


**Fig. 1** Characterisation of M1 and M2 M $\phi$ s treated with or without ZA. **a, b** Flow cytometry was used to measure the expression of CD64 and CD206 on M0, M1 and M2 M $\phi$ s treated with (orange) or without (blue) ZA for the last 18 h of culture. **a** Representative flow cytometry plots from one of six donors (–ZA). Dead cells and debris were excluded based on forward scatter (FSC) and side scatter (SSC) using gate (G) 1. Unfilled overlays = test, filled overlays = isotype. Numbers on the plots are percentage of cells within the marker. **b** Individual data points and means for six donors. Test MFIs for the total G1 population were divided by isotype controls to obtain relative MFIs. **c** M0, M1 and M2 M $\phi$ s treated with (orange) or without

(blue) ZA for the last 18 h of culture were cultured overnight in fresh medium with or without 100 ng/ml LPS. The concentration of IL-12p70 and CCL18 in culture supernatants was measured using ELISAs. Data for IL-12p70 is in the presence of LPS, whereas data for CCL18 is in the absence of LPS. Individual data points and means for six donors are shown. For **b** and **c**, data were analysed by repeated measures two-way ANOVA and comparisons between means carried out using Tukey's multiple comparison tests. \*\*\* and \*\*\*\* indicate *p* values of <0.001 and <0.0001, respectively. Statistical differences for comparisons within the +ZA (orange) data sets are not shown

washed in flow cytometry buffer and fixed in CellFIX (Becton–Dickinson). Perforin expression in V $\delta$ 2<sup>+</sup> T cells was assessed in PBMCs cultured with ZA and IL-2 for 0, 1 and 9 days as described in "Cell culture". Cells were resuspended in flow cytometry buffer containing PE-conjugated mouse anti-human V $\delta$ 2 (clone 123R3; Miltenyi Biotec) and PerCP-conjugated mouse anti-human CD3 (clone SK7; Biolegend). After 10 min at room temperature, cells were washed in flow cytometry buffer and simultaneously fixed and permeabilised using Cytofix/Cytoperm (Becton–Dickinson) according to the manufacturer's instructions. Cells were washed and resuspended in Perm/Wash buffer (Becton–Dickinson) and then labelled with FITC-conjugated mouse anti-human perforin (clone  $\delta$ G9; Becton–Dickinson) or matched isotype controls. After 10 min at room temperature, cells were washed in Perm/Wash buffer and resuspended in flow cytometry buffer. Samples were acquired on an LSR II flow cytometer (Becton–Dickinson) and analysed using FlowJo software. All comparatively analysed samples were acquired on the same day except for the time course of perforin expression where day 0, 1 and 9 samples were acquired on different days. The mean fluorescence intensity (MFI) values stated throughout are arithmetic means.

## ELISAs

Day 10 M $\phi$ s in 12-well tissue culture plates were washed twice in PBS and cultured overnight in complete medium (1 ml/well) with or without 100 ng/ml LPS (*E.coli* 0127:B8; Sigma-Aldrich). The concentration of IL-12p70 and chemokine (C–C motif) ligand (CCL) 18 within cell-free culture supernatants was determined using DuoSet ELISA kits according to the manufacturer's instructions (R and D Systems). Optical densities at 450 nm were determined using a microplate reader (Dy nex), and concentrations were extrapolated from standard curve data using a four parameter logistic model generated by GraphPad Prism 6 (GraphPad Software). Standard curves were 31.25–2000 pg/ml for IL-12p70, and 7.8125–500 pg/ml for CCL18.

## Carboxyfluorescein succinimidyl ester/Zombie-NIR cytotoxicity assay

Detaching the M $\phi$ s from the tissue culture plates prior to performing the cytotoxicity assays resulted in poor viability; therefore, cytotoxicity was assessed by adding V $\delta$ 2<sup>+</sup> T cells directly to adherent M $\phi$ s. Day 10 M $\phi$ s in 12-well tissue culture plates were washed twice in PBS and then cultured for 20 min in PBS containing 1  $\mu$ M carboxyfluorescein succinimidyl ester (CFSE; Life Technologies). M $\phi$ s were washed three times in complete medium and then cultured overnight

with or without  $1.52 \times 10^6$  autologous V $\delta$ 2<sup>+</sup> T cells per well in 2 ml complete medium to obtain an E:T ratio of 2:1 based on the initial seeding density of monocytes. For some experiments V $\delta$ 2<sup>+</sup> T cells were pre-treated for 2 h with or without 100 ng/ml concanamycin A (CMA; Abcam) or DMSO, then washed three times in complete medium prior to being cultured with M $\phi$ s. Non-adherent cells were collected and adherent cells detached from the tissue culture plates as described in "Flow cytometry". All cells were washed in PBS and then labelled with Zombie-NIR live/dead cell discrimination dye according to the manufacturer's instructions (Biolegend). Zombie-NIR binds to amine groups on proteins, but does not penetrate an intact plasma membrane. Live cells have relatively low expression because only cell surface proteins are available for binding, whereas dead cells exhibit higher levels of expression because their compromised plasma membrane permits binding to both extracellular and intracellular proteins. After 15 min at room temperature, cells were washed in complete medium and fixed in CellFIX. Samples were acquired on an LSR II flow cytometer and analysed using FlowJo software. All comparatively analysed samples were acquired on the same day.

## CD107 mobilisation assay

Day 10 M $\phi$ s in 96-well tissue culture plates were washed three times in PBS and then cultured for 5 h with  $1.52 \times 10^5$  autologous V $\delta$ 2<sup>+</sup> T cells per well in 200  $\mu$ l complete medium to obtain an E:T ratio of 2:1 based on the initial seeding density of monocytes. Allophycocyanin-conjugated mouse anti-human CD107a (clone H4A3; Biolegend) and FITC-conjugated mouse anti-human CD107b (clone H4B4; Biolegend) or matched isotype controls were added directly to the wells at the start of the co-culture along with 1  $\mu$ g/ml of monensin to neutralise intracellular acidity. Cells were then collected and labelled with PE-conjugated mouse anti-human V $\delta$ 2 (clone 123R3; Miltenyi Biotec) and PerCP-conjugated mouse anti-human CD3 (clone SK7; Biolegend) as described in "Flow cytometry". Samples were acquired on an LSR II flow cytometer and analysed using FlowJo software. All comparatively analysed samples were acquired on the same day.

## Statistical analyses

Data in Figs. 1b, c, 3b, d and 4c were analysed by repeated measures one-way or two-way ANOVA and comparisons between means carried out using either Tukey's or Sidak's multiple comparison tests (GraphPad Prism 6). \*, \*\*, \*\*\* and \*\*\*\* were used to indicate *p* values of <0.05, <0.01, <0.001 and <0.0001, respectively. Gaussian distributions were assumed. Data in Fig. 2b included a three-way (3  $\times$  2  $\times$  2) factorial design repeated six times using cells from six different donors. The three factors

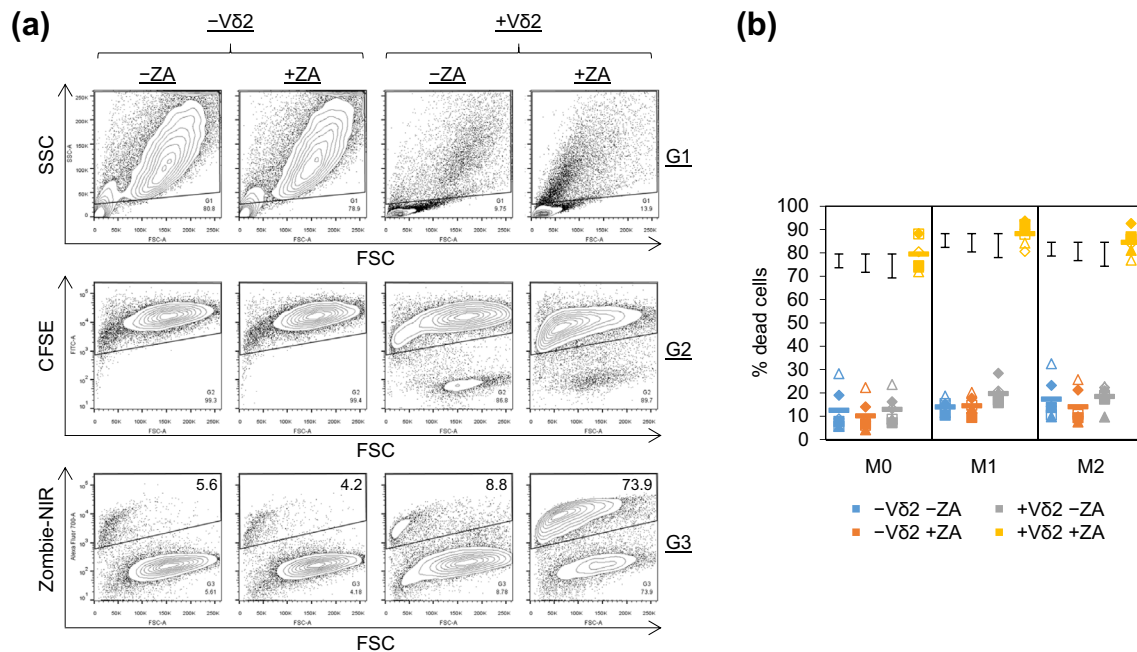


**Fig. 2**  $V\delta 2^+$  T cell cytotoxicity towards ZA-treated M1 and M2 Mφs. M0, M1 and M2 Mφs treated with or without ZA for the last 18 h of culture were labelled with CFSE and cultured overnight with or without autologous  $V\delta 2^+$  T cells. Flow cytometry was then used to measure Zombie-NIR expression. **a** Representative flow cytometry contour plots from one of six donors showing the gating strategy used to determine Zombie-NIR expression in M0 Mφs. Mφs were gated based on FSC and SSC using G1. CFSE<sup>+</sup> cells within G1

were gated using G2. The percentage of Zombie-NIR<sup>high</sup> cells (i.e. dead cells) within G1 + G2 was then determined using G3. Numbers on the contour plots are percentages of cells within G3. **b** Individual data points and means for six donors. Data were analysed by three-way ANOVA and comparisons between means carried out using Fisher's LSD tests. The 5, 1 and 0.1% LSDs are depicted by the *black* intervals

were Mφ type (M0, M1 and M2),  $\pm$ ZA and  $\pm$ V $\delta$ 2 cells. Data in Fig. 4b were a three-way ( $3 \times 2 \times 4$ ) factorial design repeated five times using cells from five different donors. The three factors were Mφ type (M0, M1 and M2),  $\pm$ ZA and  $\pm$ V $\delta$ 2 cells ( $-V\delta 2$ ,  $+V\delta 2$ ,  $+V\delta 2$ [DMSO] and  $+V\delta 2$ [CMA]). Data in Figs. 2b and 4b were analysed by three-way ANOVA and comparisons between means carried out using Fisher's least significant difference (LSD; Genstat 18). Assumptions underlying the analysis were checked using the diagnostic plots produced by the software. LSDs at the 5, 1 and 0.1% level are depicted by black intervals, and differences in the means that were greater than this interval were deemed significant to an equivalent *p* value of  $<0.05$ ,  $<0.01$  and  $<0.001$ , respectively.

## Results

### ZA did not alter M1 or M2 markers on Mφs

We differentiated monocytes from the peripheral blood of healthy donors into Mφs and treated them with IFN- $\gamma$  or

IL-4 to generate M1 and M2 Mφs, respectively. We then characterised these Mφs based on their expression of markers for M1 Mφs (CD64 and IL-12p70) and M2 Mφs (CD206 and CCL18) [19, 22]. M1 Mφs had upregulated expression of CD64, whereas M2 Mφs had downregulated CD64 and upregulated CD206 (Fig. 1a, b). Although, statistically, we observed significantly higher levels of CD206 on M1 Mφs compared with M0 Mφs in terms of percentage expression, this was not consistent for all donors and not statistically significant in terms of relative MFI (Fig. 1b). Mφs were then cultured overnight with or without LPS to measure the production of IL-12p70 and CCL18, respectively. M1 Mφs produced more IL-12p70 than M0 and M2 Mφs, whereas M2 Mφs produced more CCL18 than M0 and M1 Mφs (Fig. 1c). We also tested whether ZA—added for the last 18 h of culture—had any effect on these markers and found little or no difference between untreated and ZA-treated Mφs (Fig. 1). Taken together, these data validate our protocol for generating M1 and M2 Mφs and show that ZA does not alter the M1 and M2 profile of the Mφs in this system.

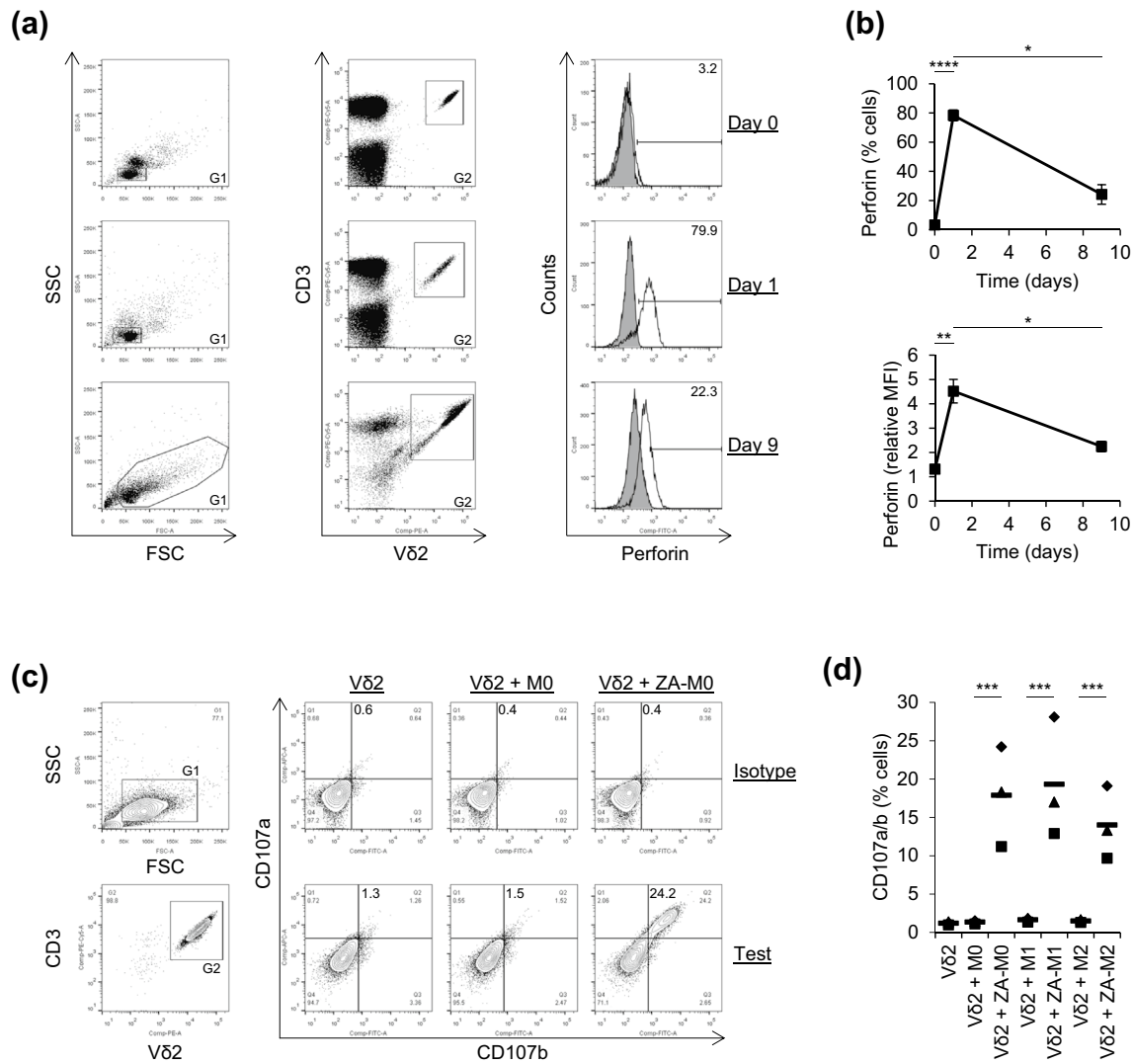


**Fig. 3** Expression of perforin and mobilisation of CD107a and CD107b in Vδ2<sup>+</sup> T cells. **a, b** Flow cytometry was used to measure the expression of perforin by Vδ2<sup>+</sup> T cells in PBMCs cultured with ZA and IL-2 for 0, 1 and 9 days. **a** Representative flow cytometry plots from one of three donors showing perforin expression in Vδ2<sup>+</sup> T cells. Lymphocytes were gated based on FSC and SSC using G1. Note that G1 was extended at day 9 to incorporate blast cells. Vδ2<sup>+</sup>CD3<sup>+</sup> cells within G1 were gated using G2. Percentage expression and MFI of perforin within G1 + G2 was then assessed. Unfilled overlays = test, filled overlays = isotype. Numbers on the histogram plots are percentage of cells within the marker. **b** Mean ± SD for three donors. Test MFIs for the total G1 + G2 population were divided by the isotype controls to obtain relative MFIs. Data were analysed by repeated measures one-way ANOVA and comparisons between means carried out using Tukey's multiple comparison tests. **c, d** Vδ2<sup>+</sup> T cells were cultured with or without autologous M0, M1

or M2 Mφs that had been treated with or without ZA for the last 18 h of culture. Flow cytometry was used to measure the expression of CD107a and CD107b by Vδ2<sup>+</sup> T cells. **c** Representative flow cytometry contour plots from one of three donors showing CD107a and CD107b expression on gated Vδ2<sup>+</sup>CD3<sup>+</sup> cells. Lymphocytes were gated based on FSC and SSC using G1. Vδ2<sup>+</sup>CD3<sup>+</sup> cells within G1 were gated using G2. Percentage expression of CD107a and CD107b within G1 + G2 was then assessed. Quadrants were set against the Vδ2 alone controls, and separate quadrants were generated for isotype and test. Numbers are percentages of cells contained within the upper right quadrants. **d** Individual data points and means for three donors. Data were analysed by repeated measures two-way ANOVA and comparisons between means carried out using Sidak's multiple comparison tests. For **b** and **d**, \*, \*\*, \*\*\* and \*\*\*\* indicate *p* values of <0.05, <0.01, <0.001 and <0.0001, respectively

### ZA-rendered M1 and M2 Mφs susceptible to Vδ2<sup>+</sup> T cell cytotoxicity

To obtain sufficient cell numbers for cytotoxicity assays, we stimulated Vδ2<sup>+</sup> T cell expansion prior to isolation.

Vδ2<sup>+</sup> T cell expansion was observed in PBMCs treated with ZA and IL-2 for 9 days, as shown by increased frequencies of Vδ2<sup>+</sup>CD3<sup>+</sup> cells (supplementary Fig. 2). Vδ2<sup>+</sup> T cells were purified by sequentially depleting dead cells and non-γδ T cells (mean ± standard deviation

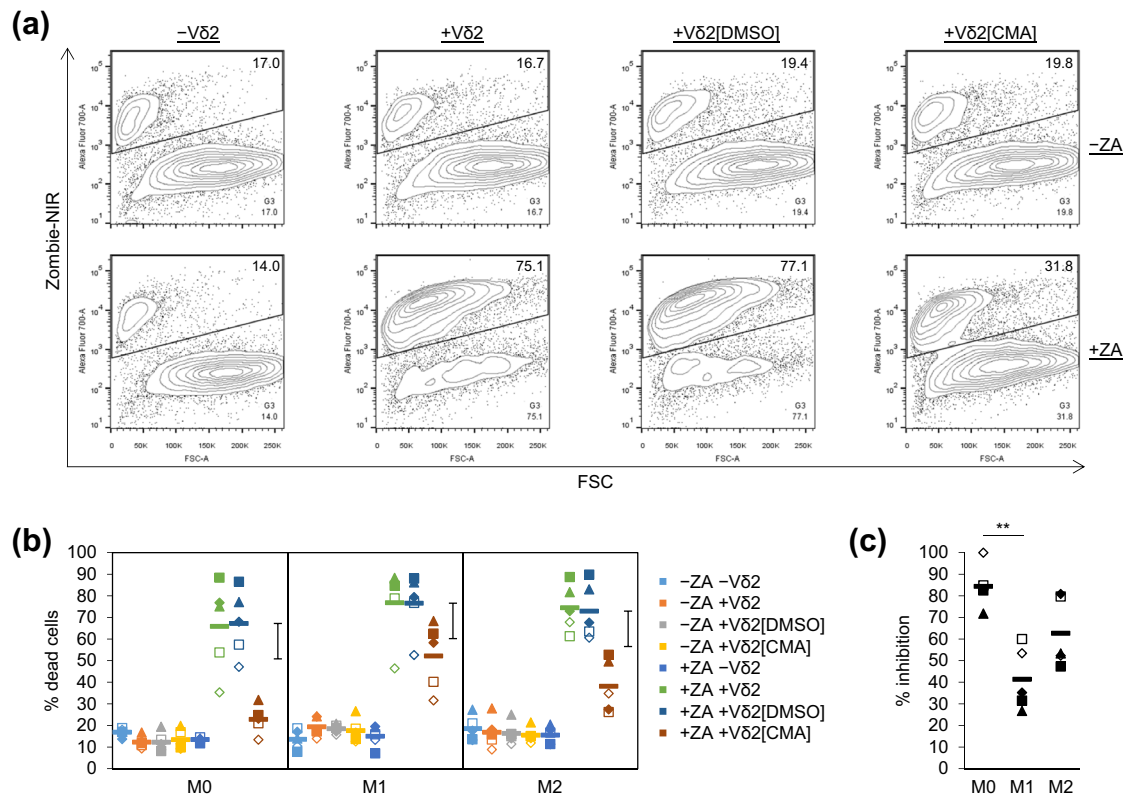


**Fig. 4** The effect of concanamycin A on  $V\delta 2^+$  T cell cytotoxicity towards ZA-treated M $\phi$ s. M0, M1 and M2 M $\phi$ s treated with or without ZA for the last 18 h of culture were labelled with CFSE and then cultured overnight with or without autologous  $V\delta 2^+$  T cells that had been pre-treated for 2 h with or without CMA (100 ng/ml) or DMSO. Flow cytometry was then used to measure Zombie-NIR expression. **a** Representative flow cytometry contour plots for M0 M $\phi$ s from one of five donors. The percentage of Zombie-NIR<sup>high</sup> cells (i.e. dead cells) within CFSE<sup>+</sup> M $\phi$ s was determined using the G1 + G2 + G3 gating strategy described in Fig. 2. Numbers on the plots are percentages of cells within G3. **b** Individual data points and means for five donors. Data were analysed by three-way ANOVA and comparisons

between means carried out using Fisher's LSD tests. The 0.1% LSD is depicted by the *black* interval. **c** Data in **b** was expressed as percentage inhibition. Within the +ZA data sets, the percentage of dead M $\phi$ s in the absence of  $V\delta 2^+$  T cells (i.e. background cell death) was subtracted from that induced by the DMSO- and CMA-treated  $V\delta 2^+$  T cells. The corrected values for M $\phi$  cell death induced by CMA-treated  $V\delta 2^+$  T cells were then expressed as a percentage of the corrected values for M $\phi$  cell death induced by DMSO-treated  $V\delta 2^+$  T cells. These values were then converted to percentage inhibition by subtracting them from 100%. Data were analysed by repeated measures one-way ANOVA and comparisons between means carried out using Tukey's multiple comparison tests. \*\* Indicates a  $p$  value <0.01

(SD) for the percentage of  $V\delta 2^+CD3^+$  cells from four donors =  $97.2 \pm 1.8$ ; supplementary Fig. 2). The percentage of  $V\delta 2^+CD3^+$  cells at day 0 and day 9 pre-depletion of dead cells and non- $\gamma\delta$  T cells was not assessed routinely; however, purities at day 9 post-depletion were assessed for all isolations performed in this study (mean  $\pm$  SD for 14 isolations =  $97.7 \pm 1.8$ ). We conducted preliminary experiments to determine the optimal E:T ratio and ZA concentration for  $V\delta 2^+$  T cell-mediated cytotoxicity against ZA-treated M $\phi$ s (supplementary Fig. 3). These experiments showed  $V\delta 2^+$  T cell cytotoxicity and degranulation against M $\phi$ s treated with 10  $\mu$ M, but not 1  $\mu$ M ZA (supplementary Fig. 3). Furthermore, they showed marked killing at the lowest E:T ratio of 2:1

(supplementary Fig. 3). Using the 10  $\mu$ M concentration of ZA and 2:1 E:T ratio, we found that ZA had little or no effect on M $\phi$  viability in the absence of  $V\delta 2^+$  T cells, and  $V\delta 2^+$  T cells did not induce cell death in M $\phi$ s that had not been treated with ZA (Fig. 2a, b). However, there was a marked increase in the amount of cell death in M $\phi$ s that were pre-treated with ZA and then cultured with  $V\delta 2^+$  T cells (Fig. 2a, b). Although, statistically,  $V\delta 2^+$  T cell-mediated killing of ZA-treated M1 M $\phi$ s was significantly higher than that of M0 M $\phi$ s, the difference was relatively small and no statistically significant difference was found between M1 and M2 M $\phi$ s (Fig. 2b). These results suggest that  $V\delta 2^+$  T cells are cytotoxic towards ZA-treated M $\phi$ s irrespective of their M0, M1 and M2 phenotype.

### V $\delta$ <sup>+</sup> T cells expressed perforin and degranulated when cultured with ZA-treated M $\phi$ s

Perforin has been shown previously to play a role in  $\gamma\delta$  T cell cytotoxicity towards tumour cell lines [23, 24]; therefore, we tested whether perforin contributes to V $\delta$ <sup>+</sup> T cell cytotoxicity towards ZA-treated M $\phi$ s. We measured perforin expression by V $\delta$ <sup>+</sup> T cells before, during and after expansion with ZA and IL-2. We found that, although resting V $\delta$ <sup>+</sup> T cells expressed little or no perforin, it was markedly upregulated after 1 day of culture with ZA and IL-2 (Fig. 3a, b). After 9 days of culture with ZA and IL-2, perforin was downregulated but still expressed by V $\delta$ <sup>+</sup> T cells (Fig. 3a, b). We also measured perforin expression in expanded and isolated V $\delta$ <sup>+</sup> T cells from six donors and found consistent expression in terms of percentage expression (mean  $\pm$  SD = 1.2  $\pm$  0.5 vs. 23.9  $\pm$  7.6 for isotype and test, respectively) and MFI (mean  $\pm$  SD = 227.8  $\pm$  15.2 vs. 490.7  $\pm$  104.6 for isotype and test, respectively). To determine if V $\delta$ <sup>+</sup> T cells release perforin when cultured with ZA-treated M $\phi$ s, we measured the mobilisation of lysosomal-associated membrane protein 1 and 2 (i.e. CD107a and CD107b) to the surface of V $\delta$ <sup>+</sup> T cells. CD107a—and to a lesser extent CD107b—was expressed on V $\delta$ <sup>+</sup> T cells that were isolated from PBMCs after 9 days of culture with ZA and IL-2 (Fig. 3c). This may represent residual CD107 expression from the monocyte-dependent degranulation that is induced when PBMCs are exposed to ZA [20]. V $\delta$ <sup>+</sup> T cells upregulated expression of CD107a and CD107b on their cell surface when cultured with ZA-treated M $\phi$ s compared with untreated M $\phi$ s (Fig. 3c, d). These data suggest that V $\delta$ <sup>+</sup> T cells express perforin and degranulate in response to ZA-treated M $\phi$ s, thus implicating a role for perforin in V $\delta$ <sup>+</sup> T cell cytotoxicity towards ZA-treated M $\phi$ s.

### V $\delta$ <sup>+</sup> T cell cytotoxicity towards ZA-treated M $\phi$ s was sensitive to concanamycin A

To explore further the potential role of perforin in V $\delta$ <sup>+</sup> T cell cytotoxicity towards ZA-treated M $\phi$ s, we repeated the cytotoxicity assays shown in Fig. 2, but this time pre-treated V $\delta$ <sup>+</sup> T cells with the H<sup>+</sup>-ATPase inhibitor CMA. CMA blocks acidification of cytolytic granules, which inhibits perforin-mediated but not Fas ligand-mediated cytotoxicity [25]. We found that pre-treating V $\delta$ <sup>+</sup> T cells with CMA reduced their cytotoxicity towards M $\phi$ s compared with DMSO controls (Fig. 4a, b). We calculated the percentage inhibition for V $\delta$ <sup>+</sup> T cell cytotoxicity towards M0, M1 and M2 M $\phi$ s and found that V $\delta$ <sup>+</sup> T cell cytotoxicity towards M0 M $\phi$ s was more sensitive to CMA than towards M1 M $\phi$ s (Fig. 4c). To determine whether CMA had an effect on V $\delta$ <sup>+</sup> T cell viability, we applied a gate

to CFSE<sup>-</sup> cells and calculated the percentage of Zombie-NIR<sup>low</sup> cells (supplementary Fig. 4a). There was a discernible reduction in V $\delta$ <sup>+</sup> T cell viability in the presence of ZA-treated M $\phi$ s compared with untreated M $\phi$ s; however, there was little or no difference in V $\delta$ <sup>+</sup> T cell viability between the CMA and DMSO treatment groups (supplementary Fig. 4b). These findings suggest that V $\delta$ <sup>+</sup> T cell cytotoxicity towards ZA-treated M $\phi$ s is sensitive—at least in part—to CMA, thus implicating a role for perforin.

## Discussion

V $\delta$ <sup>+</sup> T cells in the peripheral blood of humans are regarded as sentinels against infection [26] and malignant transformation [27]. They express the inflammatory homing receptors chemokine (C–C motif) receptor 5 and chemokine (C–X–C motif) receptor 3 [28] and thus infiltrate sites of infection [29] as well as the inflammatory microenvironment of diseased tissues such as tumours [30, 31]. M $\phi$ s are abundant in these tissues and are likely to interact closely with infiltrating V $\delta$ <sup>+</sup> T cells. We explored the potential interaction between V $\delta$ <sup>+</sup> T cells and M $\phi$ s in vitro and found that ZA can render M1 and M2 M $\phi$ s susceptible to V $\delta$ <sup>+</sup> T cell cytotoxicity in a perforin-dependent manner.

Zoledronic acid has a high affinity for hydroxyapatite [32] and thus binds rapidly to bone following i.v. infusion [33]. Therefore, the M $\phi$ s most likely to be exposed to ZA are those associated with bone and/or the surrounding tissues: for example, the TAMs in bone-related cancers such as osteosarcoma, myeloma and secondary bone metastases associated with cancers of the prostate, lung and breast. Following i.v. infusion, NBPs may also reach tissues other than bone. Intravital imaging in a murine model of breast cancer showed that a fluorescently labelled NBP—given by i.v. injection—leaked from the vasculature of mammary tumours and bound rapidly to granular microcalcifications, which were subsequently engulfed by TAMs [15]. The NBP was not retained in cells other than M $\phi$ s, nor was it retained in B16 tumours, which lack microcalcifications [15]. This study suggests that calcified tissues other than bone can also accumulate NBPs [15]. The lack of cytotoxicity and degranulation at 1  $\mu$ M ZA that was observed in our preliminary optimisation experiments suggests that the M $\phi$ s most likely to be targeted by V $\delta$ <sup>+</sup> T cells following ZA treatment are those associated with calcified tissues where the drug is likely to accumulate, which has important implications regarding the in vivo effects of this drug. It is worth noting that uptake of ZA by M $\phi$ s in vivo may be markedly different using other methods of delivery such as liposome or nanoparticle encapsulation [34, 35] and localised injection. At the cellular level, experiments conducted in vitro suggest that ZA is taken up by myeloid cells such



as monocytes, M $\phi$ s and osteoclasts via the process of fluid phase endocytosis [36, 37].

Zoledronic acid inhibits farnesyl pyrophosphate synthase of the mevalonate pathway, which has been shown *in vitro* to induce apoptosis directly in the murine M $\phi$ -like cell line J774.2 [38]. A potential mechanism for this effect is accumulation of the pro-apoptotic analogue of ATP, Apppl, which has been reported to accumulate in ZA-treated cells such as osteoclasts and MCF-7 cells [4]. Interestingly, ZA did not affect the viability of M $\phi$ s in our experiments; however, we used relatively short exposure times and did not look at markers of early stage apoptosis such as surface expression of phosphatidyl serine. Inhibition of farnesyl pyrophosphate synthase may also modulate the differentiation and function of M $\phi$ s. For example, when monocyte-derived M2 M $\phi$ s were differentiated in the presence of ZA, they had reduced expression of CD206 and IL-10, and an impaired capacity to promote angiogenesis and tumour cell invasion [39]. ZA also inhibited tumour growth in a murine model of cervical cancer, which correlated with reduced angiogenesis and decreased production of matrix metalloproteinase 9 by M $\phi$ s proximal to and associated with tumours [40]. Furthermore, ZA reduced the onset and growth of tumours in a murine model of breast cancer, which correlated with reduced vascularisation of the tumour, reduced numbers of TAMs, and repolarisation of TAMs from an M2 to M1 phenotype [41]. Taken together, these studies suggest that ZA can modulate the differentiation of M $\phi$ s towards an M1 phenotype. To the best of our knowledge, V $\delta$ 2<sup>+</sup> T cell targeting of ZA-treated M1 and M2 M $\phi$ s—as suggested by our data—has been previously unreported and broadens our understanding of the effects of ZA on M $\phi$ s. Importantly, mice do not develop the V $\delta$ 2<sup>+</sup> T cell subset that responds to ZA-induced accumulation of IPP because they lack the gene for butyrophilin 3A1 [42], thus highlighting the importance of using human cells for this study.

Our data suggests that ZA has the potential to kill M1 and M2 M $\phi$ s indirectly within tissues that are exposed to the drug and infiltrated by V $\delta$ 2<sup>+</sup> T cells. Tumours contain an abundant population of M $\phi$ s, which typically express M2 markers and correlate with a poor prognosis [43]. In breast cancer, CCL18 production by TAMs promotes angiogenesis and thus supports tumour growth and dissemination [44]. Furthermore, M2 M $\phi$ s in the bone marrow of multiple myeloma patients have been shown to protect malignant cells from chemotherapy-induced apoptosis [45, 46]. In contrast, osteosarcomas can contain relatively high percentages of M1 M $\phi$ s, which are associated with reduced metastases and improved survival [47]. The potential for ZA to render M $\phi$ s susceptible to V $\delta$ 2<sup>+</sup> T cells may be beneficial or detrimental depending on which type of M $\phi$  is present in the tumour. For example,

it may be beneficial in patients with breast cancer or myeloma and could explain the promising responses to ZA reported for clinical trials in these cancer types [48, 49], whereas it may be counterproductive in osteosarcoma.

It is important to note that our study has focussed on the killing capacity of activated V $\delta$ 2<sup>+</sup> T cells. Although it would be interesting to compare the cytotoxicity of resting and activated V $\delta$ 2<sup>+</sup> T cells, the relatively low frequency of V $\delta$ 2<sup>+</sup> T cells in peripheral blood meant that we were unable to isolate the number of resting V $\delta$ 2<sup>+</sup> T cells required to perform the cytotoxicity assays used in this study. Whether or not *i.v.* infusion of ZA—combined with *i.v.* or *s.c.* IL-2—can activate peripheral blood V $\delta$ 2<sup>+</sup> T cells *in vivo* is a point of contention. Current hypotheses state that peripheral blood monocytes take up ZA following *i.v.* infusion and subsequently activate V $\delta$ 2<sup>+</sup> T cells [37]; indeed, proliferation and/or differentiation of peripheral blood V $\delta$ 2<sup>+</sup> T cells has been reported in some patients receiving ZA and IL-2 [9–11]. However, V $\delta$ 2<sup>+</sup> T cell responses were not observed in all patients [50] and it is unclear whether this is due to lack of activation or detection. Importantly, V $\delta$ 2<sup>+</sup> T cells that are pre-activated may be more cytotoxic than resting, and thus ZA-induced targeting of M $\phi$ s by V $\delta$ 2<sup>+</sup> T cells *in vivo* may be suboptimal in patients for whom ZA and IL-2 treatment fails to activate their circulating V $\delta$ 2<sup>+</sup> T cells, thus highlighting the importance of effective V $\delta$ 2<sup>+</sup> T cell priming in the periphery.

In our study, V $\delta$ 2<sup>+</sup> T cell cytotoxicity towards M0, M1 and M2 M $\phi$ s was sensitive—at least in part—to the perforin inhibitor CMA, thus implicating a role for perforin [25]. Interestingly, CMA did not inhibit cytotoxicity completely, and the degree of inhibition varied between the different types of M $\phi$ ; specifically, V $\delta$ 2<sup>+</sup> T cell cytotoxicity towards M0 M $\phi$ s was more sensitive to CMA than towards M1 M $\phi$ s. If, in our assays, CMA blocked perforin completely, our data would suggest that other mechanisms of cell-mediated cytotoxicity are involved and that the contribution of perforin versus other mechanisms of cytotoxicity varies between the different types of M $\phi$ . Indeed, V $\delta$ 2<sup>+</sup> T cells have been shown to kill target cells through the expression of Fas ligand and TRAIL [51]. However, if perforin blockade was incomplete, the variation in sensitivity to CMA that was observed between the different types of M $\phi$  could also be attributed to differences in their susceptibility to perforin-mediated killing under conditions of suboptimal perforin activity. Nonetheless, our data suggest that perforin plays a role, which provides a useful mechanistic marker for exploring this concept *in vivo*.

In conclusion, this study sheds light on a potential interaction between V $\delta$ 2<sup>+</sup> T cells and M $\phi$ s following ZA treatment and suggests a mechanism of action for this drug that may help its future development in cancer immunotherapy.

**Acknowledgements** The authors would like to thank the Institute for Cancer Vaccines and Immunotherapy (Registered Charity Number 1080343) for funding this research. The authors would like to thank Dr. David Lovell, Reader in Medical Statistics at St. George's University of London, for his advice and expertise in performing the statistical analyses using ANOVA for the three-way factorial design.

#### Compliance with ethical standards

**Conflict of interest** The authors declare that they have no conflict of interest.

**Open Access** This article is distributed under the terms of the Creative Commons Attribution 4.0 International License (<http://creativecommons.org/licenses/by/4.0/>), which permits unrestricted use, distribution, and reproduction in any medium, provided you give appropriate credit to the original author(s) and the source, provide a link to the Creative Commons license, and indicate if changes were made.

#### References

- Morita CT, Jin C, Sarikonda G, Wang H (2007) Nonpeptide antigens, presentation mechanisms, and immunological memory of human Vgamma2Vdelta2 T cells: discriminating friend from foe through the recognition of prenyl pyrophosphate antigens. *Immunol Rev* 215:59–76
- Gober HJ, Kistowska M, Angman L, Jenö P, Mori L, De Libero G (2003) Human T cell receptor gammadelta cells recognize endogenous mevalonate metabolites in tumor cells. *J Exp Med* 197:163–168
- Kistowska M, Rossy E, Sansano S, Gober HJ, Landmann R, Mori L, De Libero G (2008) Dysregulation of the host mevalonate pathway during early bacterial infection activates human TCR gamma delta cells. *Eur J Immunol* 38:2200–2209
- Raikkonen J, Crockett JC, Rogers MJ, Monkkonen H, Auriola S, Monkkonen J (2009) Zoledronic acid induces formation of a pro-apoptotic ATP analogue and isopentenyl pyrophosphate in osteoclasts in vivo and in MCF-7 cells in vitro. *Br J Pharmacol* 157:427–435
- Kavanagh KL, Guo K, Dunford JE, Wu X, Knapp S, Ebetino FH, Rogers MJ, Russell RG, Oppermann U (2006) The molecular mechanism of nitrogen-containing bisphosphonates as antiosteoporosis drugs. *Proc Natl Acad Sci USA* 103:7829–7834
- Harly C, Guillaume Y, Nedellec S, Peigne CM, Monkkonen H, Monkkonen J, Li J, Kuball J, Adams EJ, Netzer S, Dechanet-Merville J, Leger A, Herrmann T, Breathnach R, Olive D, Bonneville M, Scotet E (2012) Key implication of CD277/butyrophilin-3 (BTN3A) in cellular stress sensing by a major human gammadelta T-cell subset. *Blood* 120:2269–2279
- Lipton A (2005) New therapeutic agents for the treatment of bone diseases. *Expert Opin Biol Ther* 5:817–832
- Benford HL, McGowan NW, Helfrich MH, Nuttall ME, Rogers MJ (2001) Visualization of bisphosphonate-induced caspase-3 activity in apoptotic osteoclasts in vitro. *Bone* 28:465–473
- Dieli F, Vermijlen D, Fulfaro F, Caccamo N, Meraviglia S, Cicero G, Roberts A, Buccheri S, D'Asaro M, Gebbia N, Salerno A, Eberl M, Hayday AC (2007) Targeting human gamma delta T cells with zoledronate and interleukin-2 for immunotherapy of hormone-refractory prostate cancer. *Cancer Res* 67:7450–7457
- Meraviglia S, Eberl M, Vermijlen D, Todaro M, Buccheri S, Cicero G, La Mendola C, Guggino G, D'Asaro M, Orlando V, Scarpa F, Roberts A, Caccamo N, Stassi G, Dieli F, Hayday AC (2010) In vivo manipulation of Vgamma9Vdelta2 T cells with zoledronate and low-dose interleukin-2 for immunotherapy of advanced breast cancer patients. *Clin Exp Immunol* 161:290–297
- Kunzmann V, Smetak M, Kimmel B, Weigang-Koehler K, Goebeler M, Birkmann J, Becker J, Schmidt-Wolf IG, Einsele H, Wilhelm M (2012) Tumor-promoting versus tumor-antagonizing roles of gammadelta T cells in cancer immunotherapy: results from a prospective phase I/II trial. *J Immunother* 35:205–213
- Wrobel P, Shojaei H, Schitteck B, Gieseler F, Wollenberg B, Kalthoff H, Kabelitz D, Wesch D (2007) Lysis of a broad range of epithelial tumour cells by human gamma delta T cells: involvement of NKG2D ligands and T-cell receptor- versus NKG2D-dependent recognition. *Scand J Immunol* 66:320–328
- Bouet-Toussaint F, Cabillie F, Toutirais O, Le Gallo M, Thomas de la Pintiere C, Daniel P, Genetet N, Meunier B, Dupont-Bierre E, Boudjema K, Catros V (2008) Vgamma-9Vdelta2 T cell-mediated recognition of human solid tumors. Potential for immunotherapy of hepatocellular and colorectal carcinomas. *Cancer Immunol Immunother* 57:531–539
- Saitoh A, Narita M, Watanabe N, Tochiki N, Satoh N, Takizawa J, Furukawa T, Toba K, Aizawa Y, Shinada S, Takahashi M (2008) Anti-tumor cytotoxicity of gammadelta T cells expanded from peripheral blood cells of patients with myeloma and lymphoma. *Med Oncol* 25:137–147
- Junankar S, Shay G, Jurczyk J, Ali N, Down J, Pocock N, Parker A, Nguyen A, Sun S, Kashemirov B, McKenna CE, Croucher PI, Swarbrick A, Weilbaecher K, Phan TG, Rogers MJ (2015) Real-time intravital imaging establishes tumor-associated macrophages as the extraskelatal target of bisphosphonate action in cancer. *Cancer Discov* 5:35–42
- Mills CD, Lenz LL, Harris RA (2016) A breakthrough: macrophage-directed cancer immunotherapy. *Cancer Res* 76:513–516
- Murray PJ, Wynn TA (2011) Protective and pathogenic functions of macrophage subsets. *Nat Rev Immunol* 11:723–737
- Biswas SK, Mantovani A (2010) Macrophage plasticity and interaction with lymphocyte subsets: cancer as a paradigm. *Nat Immunol* 11:889–896
- Murray PJ, Allen JE, Biswas SK, Fisher EA, Gilroy DW, Goerdt S, Gordon S, Hamilton JA, Ivashkiv LB, Lawrence T, Locati M, Mantovani A, Martinez FO, Mege JL, Mosser DM, Natoli G, Saeij JP, Schultze JL, Shirey KA, Sica A et al (2014) Macrophage activation and polarization: nomenclature and experimental guidelines. *Immunity* 41:14–20
- Fowler DW, Copier J, Dalgleish AG, Bodman-Smith MD (2014) Zoledronic acid causes gammadelta T cells to target monocytes and down-modulate inflammatory homing. *Immunology* 143:539–549
- Wahl LM, Wahl SM, Smythies LE, Smith PD (2006) Isolation of human monocyte populations. *Curr Protoc Immunol*. Chapter 7: Unit 7.6A
- Ambarus CA, Krausz S, van Eijk M, Hamann J, Radstake TR, Reedquist KA, Tak PP, Baeten DL (2012) Systematic validation of specific phenotypic markers for in vitro polarized human macrophages. *J Immunol Methods* 375:196–206
- Alexander AA, Maniar A, Cummings JS, Hebbeler AM, Schulze DH, Gastman BR, Pauza CD, Strome SE, Chapoval AI (2008) Isopentenyl pyrophosphate-activated CD56 + gamma delta T lymphocytes display potent antitumor activity toward human squamous cell carcinoma. *Clin Cancer Res* 14:4232–4240
- Mattarollo SR, Kenna T, Nieda M, Nicol AJ (2007) Chemotherapy and zoledronate sensitize solid tumour cells to Vgamma9Vdelta2 T cell cytotoxicity. *Cancer Immunol Immunother* 56:1285–1297

25. Kataoka T, Shinohara N, Takayama H, Takaku K, Kondo S, Yonehara S, Nagai K (1996) Concanamycin A, a powerful tool for characterization and estimation of contribution of perforin- and Fas-based lytic pathways in cell-mediated cytotoxicity. *J Immunol* 156:3678–3686
26. Dieli F, Troye-Blomberg M, Farouk SE, Sireci G, Salerno A (2001) Biology of gammadelta T cells in tuberculosis and malaria. *Curr Mol Med* 1:437–446
27. Fowler DW, Bodman-Smith MD (2015) Harnessing the power of Vdelta2 cells in cancer immunotherapy. *Clin Exp Immunol* 180:1–10
28. Glatzel A, Wesch D, Schiemann F, Brandt E, Janssen O, Kabelitz D (2002) Patterns of chemokine receptor expression on peripheral blood gamma delta T lymphocytes: strong expression of CCR5 is a selective feature of V delta 2/V gamma 9 gamma delta T cells. *J Immunol* 168:4920–4929
29. Liuzzi AR, Kift-Morgan A, Lopez-Anton M, Friberg IM, Zhang J, Brook AC, Roberts GW, Donovan KL, Colmont CS, Toleman MA, Bowen T, Johnson DW, Topley N, Moser B, Fraser DJ, Eberl M (2016) Unconventional human T cells accumulate at the site of infection in response to microbial ligands and induce local tissue remodeling. *J Immunol* 197:2195–2207
30. Cordova A, Toia F, La Mendola C, Orlando V, Meraviglia S, Rinaldi G, Todaro M, Cicero G, Zichichi L, Donni PL, Caccamo N, Stassi G, Dieli F, Moschella F (2012) Characterization of human gammadelta T lymphocytes infiltrating primary malignant melanomas. *PLoS ONE* 7:e49878
31. Bank I, Book M, Huszar M, Baram Y, Schnirer I, Brenner H (1993) V delta 2 + gamma delta T lymphocytes are cytotoxic to the MCF 7 breast carcinoma cell line and can be detected among the T cells that infiltrate breast tumors. *Clin Immunol Immunopathol* 67:17–24
32. Lawson MA, Xia Z, Barnett BL, Triffitt JT, Phipps RJ, Dunford JE, Locklin RM, Ebetino FH, Russell RG (2010) Differences between bisphosphonates in binding affinities for hydroxyapatite. *J Biomed Mater Res B Appl Biomater* 92:149–155
33. Kimmel DB (2007) Mechanism of action, pharmacokinetic and pharmacodynamic profile, and clinical applications of nitrogen-containing bisphosphonates. *J Dent Res* 86:1022–1033
34. Marra M, Salzano G, Leonetti C, Porru M, Franco R, Zappavigna S, Liguori G, Botti G, Chieffi P, Lamberti M, Vitale G, Abbruzzese A, La Rotonda MI, De Rosa G, Caraglia M (2012) New self-assembly nanoparticles and stealth liposomes for the delivery of zoledronic acid: a comparative study. *Biotechnol Adv* 30:302–309
35. Schiraldi C, Zappavigna S, D'Agostino A, Porto S, Gaito O, Lusa S, Lamberti M, De Rosa M, De Rosa G, Caraglia M (2014) Nanoparticles for the delivery of zoledronic acid to prostate cancer cells: a comparative analysis through time lapse video-microscopy technique. *Cancer Biol Ther* 15:1524–1532
36. Thompson K, Rogers MJ, Coxon FP, Crockett JC (2006) Cytosolic entry of bisphosphonate drugs requires acidification of vesicles after fluid-phase endocytosis. *Mol Pharmacol* 69:1624–1632
37. Roelofs AJ, Jauhainen M, Monkkinen H, Rogers MJ, Monkkinen J, Thompson K (2009) Peripheral blood monocytes are responsible for gammadelta T cell activation induced by zoledronic acid through accumulation of IPP/DMAPP. *Br J Haematol* 144:245–250
38. Rogers TL, Wind N, Hughes R, Nutter F, Brown HK, Vasiliadou I, Ottewill PD, Hohen I (2013) Macrophages as potential targets for zoledronic acid outside the skeleton-evidence from in vitro and in vivo models. *Cell Oncol (Dordr)* 36:505–514
39. Comito G, Segura CP, Taddei ML, Lanciotti M, Serni S, Morandi A, Chiarugi P, Giannoni E (2017) Zoledronic acid impairs stromal reactivity by inhibiting M2-macrophages polarization and prostate cancer-associated fibroblasts. *Oncotarget* 8:118–132
40. Giraudo E, Inoue M, Hanahan D (2004) An amino-bisphosphonate targets MMP-9-expressing macrophages and angiogenesis to impair cervical carcinogenesis. *J Clin Invest* 114:623–633
41. Coscia M, Quagliano E, Iezzi M, Curcio C, Pantaleoni F, Riganti C, Hohen I, Monkkinen H, Boccadoro M, Forni G, Musiani P, Bosia A, Cavallo F, Massaia M (2010) Zoledronic acid repolarizes tumour-associated macrophages and inhibits mammary carcinogenesis by targeting the mevalonate pathway. *J Cell Mol Med* 14:2803–2815
42. Karunakaran MM, Gobel TW, Starick L, Walter L, Herrmann T (2014) Vgamma9 and Vdelta2 T cell antigen receptor genes and butyrophilin 3 (BTN3) emerged with placental mammals and are concomitantly preserved in selected species like alpaca (*Vicugna pacos*). *Immunogenetics* 66:243–254
43. Schmieder A, Michel J, Schonhaar K, Goerdts S, Schledzewski K (2012) Differentiation and gene expression profile of tumor-associated macrophages. *Semin Cancer Biol* 22:289–297
44. Lin L, Chen YS, Yao YD, Chen JQ, Chen JN, Huang SY, Zeng YJ, Yao HR, Zeng SH, Fu YS, Song EW (2015) CCL18 from tumor-associated macrophages promotes angiogenesis in breast cancer. *Oncotarget* 6:34758–34773
45. Beider K, Bitner H, Leiba M, Gutwein O, Koren-Michowitz M, Ostrovsky O, Abraham M, Wald H, Galun E, Peled A, Nagler A (2014) Multiple myeloma cells recruit tumor-supportive macrophages through the CXCR4/CXCL12 axis and promote their polarization toward the M2 phenotype. *Oncotarget* 5:11283–11296
46. Zheng Y, Cai Z, Wang S, Zhang X, Qian J, Hong S, Li H, Wang M, Yang J, Yi Q (2009) Macrophages are an abundant component of myeloma microenvironment and protect myeloma cells from chemotherapy drug-induced apoptosis. *Blood* 114:3625–3628
47. Buddingh EP, Kuijjer ML, Duim RA, Burger H, Agelopoulos K, Myklebost O, Serra M, Mertens F, Hogendoorn PC, Lankester AC, Cleton-Jansen AM (2011) Tumor-infiltrating macrophages are associated with metastasis suppression in high-grade osteosarcoma: a rationale for treatment with macrophage activating agents. *Clin Cancer Res* 17:2110–2119
48. Aviles A, Neri N, Huerta-Guzman J, Nambo MJ (2013) Randomized clinical trial of zoledronic acid in multiple myeloma patients undergoing high-dose chemotherapy and stem-cell transplantation. *Curr Oncol* 20:e13–e20
49. Valachis A, Polyzos NP, Coleman RE, Gnant M, Eidtmann H, Brufsky AM, Aft R, Tevaarwerk AJ, Swenson K, Lind P, Mauri D (2013) Adjuvant therapy with zoledronic acid in patients with breast cancer: a systematic review and meta-analysis. *Oncologist* 18:353–361
50. Lang JM, Kaikobad MR, Wallace M, Staab MJ, Horvath DL, Wilding G, Liu G, Eickhoff JC, McNeel DG, Malkovsky M (2011) Pilot trial of interleukin-2 and zoledronic acid to augment gammadelta T cells as treatment for patients with refractory renal cell carcinoma. *Cancer Immunol Immunother* 60:1447–1460
51. Li H, Xiang Z, Feng T, Li J, Liu Y, Fan Y, Lu Q, Yin Z, Yu M, Shen C, Tu W (2013) Human Vgamma9Vdelta2-T cells efficiently kill influenza virus-infected lung alveolar epithelial cells. *Cell Mol Immunol* 10:159–164